Chinese Journal of Natural Medicines

Identification and biomimetic synthesis of iphionanes and cyperanes from *Artemisia hedinii* and their anti-hepatic fibrosis activity

Xiaofei Liu, Xing Wang, Chunping Tang, Changqiang Ke, Bintao Hu, Sheng Yao, Yang Ye

Citation: Xiaofei Liu, Xing Wang, Chunping Tang, Changqiang Ke, Bintao Hu, Sheng Yao, Yang Ye, Identification and biomimetic synthesis of iphionanes and cyperanes from *Artemisia hedinii* and their anti-hepatic fibrosis activity, Chinese Journal of Natural Medicines, 2025, 23(7), 871-880. doi: 10.1016/S1875-5364(25)60915-0.

View online: https://doi.org/10.1016/S1875-5364(25)60915-0

Chinese Journal of Natural Medicines 23 (2025) 871-880

Contents lists available at ScienceDirect

Chinese Journal of Natural Medicines

journal homepage: www.cjnmcpu.com/

Original article

Identification and biomimetic synthesis of iphionanes and cyperanes from *Artemisia hedinii* and their anti-hepatic fibrosis activity

Xiaofei Liu[a,b,Δ], Xing Wang[a,b,Δ], Chunping Tang[a], Changqiang Ke[a], Bintao Hu[a,*], Sheng Yao[a,b,c,*], Yang Ye[a,b,d,*]

[a] *State Key Laboratory of Drug Research & Natural Products Research Center, Shanghai Institute of Materia Medica, Chinese Academy of Sciences, Shanghai 201203, China*
[b] *School of Pharmacy, University of Chinese Academy of Sciences, Beijing 100049, China*
[c] *Zhongshan Institute for Drug Discovery, Shanghai Institute of Materia Medica, Chinese Academy of Sciences, Zhongshan 528400, China*
[d] *School of Life Science and Technology, Shanghai Tech University, Shanghai 201210, China*

ARTICLE INFO

Article history:
Received 14 August 2024
Revised 7 November 2024
Accepted 11 January 2025
Available online 20 July 2025

Keywords:
Artemisia hedinii
Iphionane
Cyperane
New skeleton
Biomimetic synthesis
Anti-hepatic fibrosis

ABSTRACT

Two novel skeleton sesquiterpenoids (**1** and **6**), along with four new iphionane-type sesquiterpenes (**2**–**5**) and six new cyperane-type sesquiterpenes (**7**–**11**), were isolated from the whole plant of *Artemisia hedinii* (*A. hedinii*). The two novel skeleton compounds (**1** and **6**) were derived from the decarbonization of iphionane and cyperane-type sesquiterpenes, respectively. Their structures were elucidated through a comprehensive analysis of spectroscopic data, including high-resolution electrospray ionization mass spectrometry (HR-ESI-MS) and 1D and 2D nuclear magnetic resonance (NMR) spectra. The absolute configurations were determined using electronic circular dichroism (ECD) spectra, single-crystal X-ray crystallographic analyses, time-dependent density functional theory (TDDFT) ECD calculation, density functional theory (DFT) NMR calculations, and biomimetic syntheses. The biomimetic syntheses of the two novel skeletons (**1** and **6**) were inspired by potential biogenetic pathways, utilizing a predominant eudesmane-type sesquiterpene (**A**) in *A. hedinii* as the substrate. All compounds were evaluated in LX-2 cells for their anti-hepatic fibrosis activity. Compounds **2**, **8**, and **10** exhibited significant activity in downregulating the expression of *α*-smooth muscle actin (*α*-SMA), a protein involved in hepatic fibrosis.

1. Introduction

Sesquiterpenes demonstrate various biological activities, including anti-inflammatory, anti-tumor, anti-malarial, and immunomodulatory effects [1]. Among these, iphionane-type and cyperane-type sesquiterpenes are rare and characterized by a 5/6 fused carbocyclic skeleton. These sesquiterpenes were initially discovered in *Iphiona scabra* in 1987 [2]. To date, only eight iphionane-type sesquiterpenes [3-6] and eight cyperane-type sesquiterpenes [7-12] have been identified in natural plants, with the majority of iphionane-type sesquiterpenes being isolated from the Compositae family. Additionally, several plausible biosynthetic pathways for these two unique types of sesquiterpenes have been proposed before our research [2, 13].

Artemisia is one of the largest genera in the Compositae family, comprising approximately 1000 species. *Artemisia* species are renowned for their diverse bioactive constituents, particularly sesquiterpenes [14]. *Artemisia hedinii* (*A. hedinii*), an annual herb within the genus *Artemisia*, has been traditionally utilized as a folk medicine in the Qinghai and Gansu Provinces of China, owing to its heat-clearing, detoxifying, and anti-inflammatory properties. In a previous study, 31 eudesmane-type sesquiterpenes were isolated from *A. hedinii*, some of which demonstrated significant downregulation of IL-2 and TNF-α levels, suggesting potential anti-inflammatory effects [15, 16].

Furthermore, *A. hedinii* has been traditionally employed in the treatment of hepatobiliary disorders [17]. Hepatic fibrosis can develop from virtually all chronic liver diseases, with *α*-smooth muscle actin (*α*-SMA) serving as a crucial detection marker highly expressed in fibroblasts. A 2023 study revealed that the expression of *TRPV1* messenger ribonucleic acid (mRNA), an indicator of hepatic stellate cell (HSC) activation, negatively correlated with *α*-SMA expression [18]. These findings sparked our interest in identifying anti-hepatic fibrosis compounds that reduce the expression level of *α-SMA* mRNA, particularly in plants such as *A. hedinii*.

A comprehensive investigation of *A. hedinii* was conducted, resulting in the isolation of 11 novel sesquiterpenoids (Fig. 1). The structural elucidation of these compounds involved a thorough analysis of 1D and 2D nuclear magnetic resonance (NMR) spectroscopy, high-resolution electrospray ionization mass spectrometry (HR-ESI-MS) data, electronic circular dichroism (ECD) spectra, and single-crystal X-ray diffraction patterns. Furthermore, density functional theory (DFT) NMR calculations and biomimetic synthesis were utilized to corroborate the proposed

* Corresponding author.
E-mail addresses: hubintao@simm.ac.cn (B. Hu); yaosheng@simm.ac.cn (S. Yao); yye@simm.ac.cn (Y. Ye)
Δ These authors contributed equally to this work.

https://doi.org/10.1016/S1875-5364(25)60915-0

structures. Considering the traditional medicinal applications of *A. hedinii*, all isolated compounds were evaluated for their potential anti-hepatic fibrosis activity by measuring the relative expression levels of *α-SMA* mRNA in transforming growth factor β (TGF-β)-induced LX-2 cells.

2. Results and discussion

2.1. Structure identification and biomimetic synthesis of iphionane-type sesquiterpenes

Compound **1** was isolated as a colorless oil. Its deprotonated molecular ion at *m/z* 297.1332 ([M − H]$^-$, Calcd. for $C_{15}H_{21}O_6$, 297.1338) in the HR-ESI-MS and the ^{13}C NMR data indicated a molecular formula of $C_{15}H_{22}O_6$ with five indices of hydrogen deficiency. The infrared (IR) spectrum exhibited absorption bands at 3445, 1731, and 1714 cm^{-1}, suggesting the presence of hydroxy and carbonyl groups. The ^{1}H NMR data (Table 1) revealed signals for one oxygenated methine (δ_H 4.67) and three methyl groups (δ_H 2.19, 2.08, 1.04). The ^{13}C NMR and DEPT spectra (Table 1) resolved 15 carbon resonances, attributed to three methyls, four methylenes, three methines, and five quaternary carbons (including three carbonyl and one oxygenated). The heteronuclear multiple bond correlation (HMBC) (Fig. 2) from H_3-2′ (δ_H 2.08) to C-1′ (δ_C 171.2) and from H-9 (δ_H 4.67) to C-1′ (δ_C 171.2) indicated an acetoxyl group located at C-9. The remaining 13 carbon signals suggested that the nucleus skeleton deviated from a typical 15-carbon sesquiterpene. The ^{1}H–^{1}H correlation spectroscopy (COSY) correlations (Fig. 2) between H_2-1/H_2-2/H-3, and H_2-6/H-7/H_2-8/H-9, combined with the HMBC (Fig. 2) from H_3-14 (δ_H 1.04) to C-1 (δ_C 33.2), C-5 (δ_C 82.0), C-9 (δ_C 73.3), and C-10 (δ_C 50.5), from H_3-15 (δ_H 2.19) to C-3 (δ_C 54.5) and C-4 (δ_C 213.4), from H_2-6 (δ_H 2.15, 1.76) to C-11 (δ_C 178.8), from H_2-8 (δ_H 2.01, 1.72) to C-11 (δ_C 178.8), and from H-3 (δ_H 3.12) to C-5 (δ_C 82.0) and C-6 (δ_C 33.3), ultimately established a planar structure of 5-hydroxy-9-acetoxyiphone-4-one-12,13-dinor-11-oic acid. This compound features a previously unreported carbon skeleton, formed *via* the structural rearrangement and loss of one carbon unit from the canonical iphionane-type sesquiterpene backbone.

The nuclear Overhauser effect spectroscopy (NOESY) experiment was conducted to determine the relative configuration of compound **1**. Clear correlations between H-3/H-9 and H-7/H-9 (Fig. 3) were observed. The H-3/H-9 correlation indicated that these two protons were positioned on the same face. However, the H-7/H-9 correlation did not yield a definitive conclusion due to the protons' location on different rings.

To determine its relative and absolute configuration, a biomimetic synthesis was conducted starting from 9*β*-acetoxy-4,5-dehydro-4(15)-dihydrocostic acid (**A**), a known compound isolated from *Artemisia tournefortiana* [19], which is abundant in this plant (Scheme 1). The absolute configuration of compound **A** was determined as 7*S*,9*S*,10*S* (Supporting information). Initially, compound **A** underwent oxidation using ruthenium(III) chloride and sodium periodate in a mixed solvent of dichloromethane, acetone, acetonitrile, and water at room temperature. This oxidative cleavage process resulted in the formation of **1a** by breaking the cyclic double bond. Subsequently, **1a** was protected through methyl esterification and then reacted with potassium *tert*-butoxide at −78 °C, leading to intramolecular aldol condensation and formation of **1b**. Finally, compound **1b** was subjected to further reaction with ruthenium(III) chloride and sodium periodate at room temperature, resulting in the oxidation of the double bond in the side chain accompanied by decarboxylation, ultimately yielding compound **1**.

The biomimetic synthesis demonstrated that the stereochemistry at C-7, C-9, and C-10 remained unaltered during the synthesis of compound **1** from compound **A**. Additionally, in the intramolecular aldol condensation reaction of **1a**, the negative ion at C-3 preferentially attacks the C-5 carbon from the side with lower steric hindrance, resulting in the co-facial orientation of Me-14 and OH-5. This elucidation aligns with the previously observed NOESY correlation of H-3/H-9, which is only possible when Me-14 and OH-5 are on the same face. Furthermore, time-dependent density functional theory (TDDFT) ECD calculations performed on the proposed structure of **1** yielded a calculated ECD spectrum that closely matched the experimental spectrum (Fig. 4). Consequently, the structure of compound **1** was determined to be (3*S*,5*S*,7*R*,9*S*,10*R*)-5-hydroxy-9-acetoxyiphion-12,13-dinor-4-one-11-oic acid.

Compound **2** was isolated as a colorless oil. Its deprotonated molecular ion at *m/z* 323.1496 ([M − H]$^-$, Calcd. for $C_{17}H_{23}O_6$, 323.1495) in the HR-ESI-MS and the ^{13}C NMR data indicated a molecular formula of $C_{17}H_{24}O_6$ with six indices of hydrogen defi-

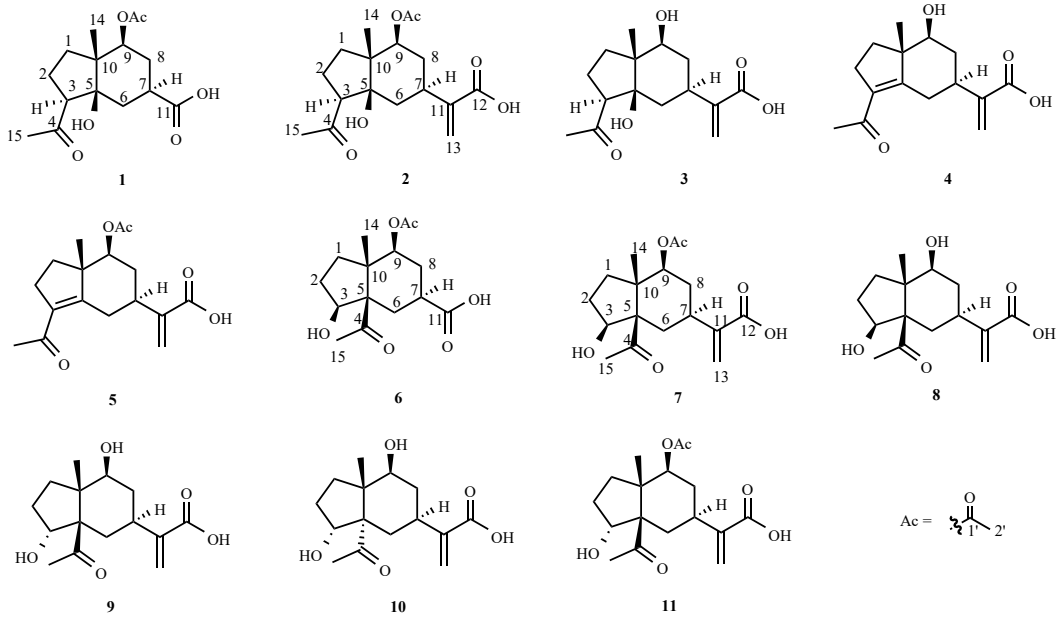

Fig. 1 Chemical structures of compounds **1**–**11**.

Table 1 ^{1}H and ^{13}C NMR data for compounds **1**–**3** in $CDCl_3$.

No.	**1**		**2**		**3**	
	δ_H (J in Hz)[a]	δ_C[c]	δ_H (J in Hz)[a]	δ_C[d]	δ_H (J in Hz)[b]	δ_C[d]
1	2.15[e] 1.65, m	33.2, t	1.78–1.63, m	33.4, t	1.98, td (12.5, 2.8) 1.63, ddd (12.5, 11.3, 7.8)	33.8, t
2	2.15[e] 1.94, dddd (13.1, 10.8, 9.4, 3.7)	24.3, t	2.13, m 1.91–2.02[e]	24.5, t	2.22[e] 1.89, m	23.3, t
3	3.12, dd (10.8, 9.4)	54.5, d	3.37, t (10.0)	54.6, d	3.37, t (9.2)	57.6, d
4		213.4, s		214.1, s		212.7, s
5		82.0, s		82.8, s		84.9, s
6	2.15[e] 1.76, m	33.3, t	1.91–2.02[e] 1.51[e]	36.9, t	2.12, ddd (12.9, 3.4, 1.9) 1.43, dd (12.9)	37.9, t
7	2.47, tt (12.9, 3.8)	37.6, d	2.69, tt (12.9, 3.2)	32.7, d	2.79, tt (12.9, 3.4)	34.2, d
8	2.01, dt (12.9, 4.3) 1.72, m	28.9, t	1.85, br d (12.9) 1.51[e]	32.1, t	1.78, dtt (12.9, 4.2, 2.9) 1.52, q (12.9)	36.2, t
9	4.67, dd (12.9, 4.3)	73.3, d	4.79, dd (12.9, 4.2)	74.3, d	3.55, dd (12.9, 4.2)	72.1, d
10		50.5, s		50.8, s		54.2, s
11		178.8, s		142.6, s[f]		146.1, s[f]
12				171.4, s[f]		170.3, s[f]
13			6.36, s 5.68, s	126.0, t	6.22, s 5.64, s	123.6, t
14	1.04, s	12.3, q	1.05, s	12.6, q	0.92, s	12.3, q
15	2.19, s	31.3, q	2.23, s	31.7, q	2.22, s	31.4, q
1′		171.2, s		171.2, s		
2′	2.08, s	21.3, q	2.08, s	21.3, q		

[a] measured at 500 MHz; [b] measured at 600 MHz; [c] measured at 150 MHz; [d] measured at 125 MHz; [e] overlapped; [f] signals identified from HMBC spectrum.

ciency. The NMR data (Table 1) were nearly identical to those of **1**, except for the signals corresponding to an additional double bond (δ_H 6.36, 5.68; δ_C 142.6, 126.0), suggesting that compound **2** might be a typical iphionane-type sesquiterpene. Although the ^{13}C NMR spectrum displayed only 15 carbon signals, the two missing carbon signals were identified through HMBC (Fig. 2) from H_3-13 (δ_H 6.36, 5.68) to C-7 (δ_C 32.7), C-11 (δ_C 142.6) and C-12 (δ_C 171.4). The spin systems inferred from the ^{1}H–^{1}H COSY spectrum (Fig. 2) revealed spin systems H_2-1/H_2-2/H-3 and H_2-6/H-7/H_2-8/H-9. HMBC (Fig. 2) from H_3-14 (δ_H 1.05) to C-1 (δ_C 33.4), C-5 (δ_C 82.8), C-9 (δ_C 74.3), and C-10 (δ_C 50.8), from H_3-15 (δ_H 2.23) to C-3 (δ_C 54.6) and C-4 (δ_C 214.1), from H_2-13 (δ_H 6.36, 5.68) to C-7 (δ_C 32.7), C-11 (δ_C 142.6) and C-12 (δ_C 171.4), and from H_3-2′ (δ_H 2.08) to C-1′ (δ_C 171.2), from H-9 (δ_H 4.79) to C-1′ (δ_C 171.2), established the planar structure of compound **2**. The NOESY spectrum exhibited correlations of H-3/H-9 and H-7/H-9, consistent with those of **1** (Fig. 3). Given the biogenetic relationship, compound **2** was postulated to be the biosynthetic precursor of compound **1**. To validate this hypothesis, a conversion reaction was performed. A methyl ester product of **2** (compound **2'**) was synthesized, which exhibited identical ^{1}H and ^{13}C NMR signals to the intermediate **1b** described in Scheme 1 (Supporting information Figs. S105, S106, S109, S110). Furthermore, the calculated ECD spectrum of **2** with the proposed structure closely matched the experimental spectrum (Fig. 4), corroborating the structural elucidation. Consequently, compound **2** was characterized as (3*S*,5*S*,7*R*,9*S*,10*R*)-5-hydroxy-9-acetoxyiphio-4-one-11(13)-en-12-oic acid.

Compound **3** was isolated as a colorless oil. Its molecular formula was determined to be $C_{15}H_{20}O_3$ based on HR-ESI-MS and ^{13}C NMR data. Compounds **3** and **2** exhibited striking similarities in their ^{1}H and ^{13}C NMR spectra (Table 1), except for the absence of acetoxyl group signals (δ_H 2.08, δ_C 171.2, 21.3) in **3**. This observation suggested that **3** might be a deacetyl derivative of **2**. The ^{1}H–^{1}H COSY and HMBC (Fig. 2), along with the ECD spectrum (Fig. 4), showing very similar Cotton effects to the calculated one, further support such elucidation. Therefore, compound **3** was identified as (3*S*,5*S*,7*R*,9*S*,10*R*)-5,9-dihydroxyiphio-4-one-11(13)-en-12-oic acid.

Compound **4** was isolated as a colorless oil and possessed a molecular formula of $C_{15}H_{20}O_4$, as determined by HR-ESI-MS data and ^{13}C NMR (Table 2). Detailed NMR data analysis revealed that **4** was also an analog of **2**. A comparison of their NMR data showed two olefinic carbons (δ_C 158.4, 134.3) instead of one methine and one oxygenated quaternary carbon at C-3 and C-5 in **2**, indicating a double bond at C-3/C-5. This elucidation was corroborated by HMBC (Fig. 2) from H_3-15 (δ_H 2.25) to C-3 (δ_C 134.3) and C-4 (δ_C 199.6), and from H_3-14 (δ_H 1.08) to C-5 (δ_C 158.4). Furthermore, signals of the acetyl group at C-9 were absent in compound **4**, suggesting a hydroxy group rather than an acetoxy group at C-9. The relative configurations of C-7, C-9, and C-10 were inferred from the NOESY correlation of H-7/H-9, H_3-

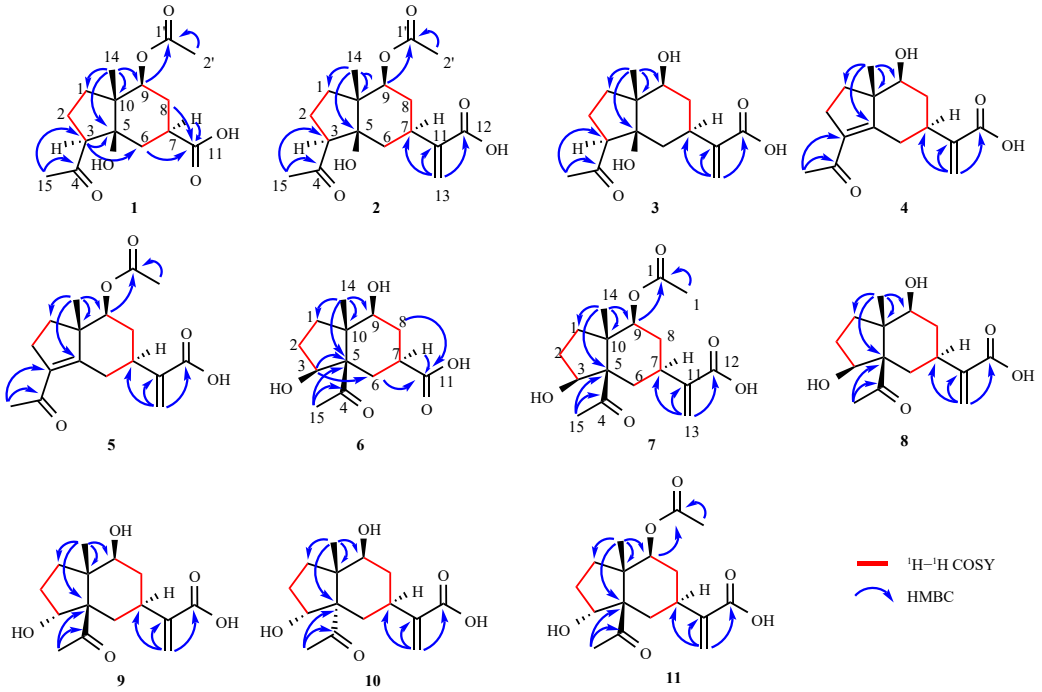

Fig. 2 Key HMBC and ^{1}H–^{1}H COSY correlations of compounds **1**–**11**.

14/H_2-1b (δ_H 1.88) and H-9/H-1a (δ_H 1.82). Considering the biogenetic relationship, compound **4** was proposed as (7*S*,9*S*,10*S*)-9-hydroxyiphio-3(5),11(13)-dien-4-one-12-oic acid. TDDFT ECD calculation conducted on the established structure of **4** showed high similarity between the calculated and experimental spectra (Fig. 5), further supporting the structural determination.

Compound **5** was isolated as a colorless oil and assigned a molecular formula of $C_{17}H_{22}O_5$, corresponding to five indices of hydrogen deficiency. Its ^{1}H and ^{13}C NMR data (Table 2) closely resembled those of **4**, with the notable addition of signals indicative of an acetyl group (δ_H 2.07, δ_C 170.7, 21.4). This suggests that **5** may be an acetyl derivative of **4**. Based on biogenetic considerations, compound **5** was hypothesized to share the same configuration as **4**. The NOESY spectrum, revealing a correlation between H-7 and H-9, and the experimental ECD spectrum, exhibiting similar Cotton effects to the calculated spectrum of **4** (Fig. 5), further supported this hypothesis. Consequently, the structure of **5** was proposed as (7*S*,9*S*,10*S*)-9-acetoxyiphio-3(5),11(13)-dien-4-one-12-oic acid.

2.2. Structure identification and biomimetic synthesis of cyperane-type sesquiterpenes

The molecular formula of **6** was determined to be $C_{15}H_{22}O_6$ based on HR-ESI-MS and ^{13}C NMR data (Table 3), indicating five indices of hydrogen deficiency. The ^{1}H NMR data (Table 3) revealed two oxygenated methines (δ_H 4.63, 4.38) and three methyls (δ_H 2.23, 2.08, 1.00). The ^{13}C NMR data (Table 3) exhibited 15 resonances attributed to three methyls (δ_C 31.9, 21.3, 15.6), four methylenes (δ_C 33.0, 31.2, 29.1, 27.7), three methines (δ_C 76.1, 73.3, 37.4), and five quaternary carbons (δ_C 213.2, 178.5, 171.0, 65.3, 47.1). An acetoxyl group at C-9 was deduced from the HMBC (Fig. 2) between H_3-2′ (δ_H 2.08) and C-1′ (δ_C 171.0), and between H-9 (δ_H 4.63) and C-1′ (δ_C 171.0). The HMBC (Fig. 2) from H_2-6 (δ_H 2.40–2.99, 2.03–2.10) to C-11 (δ_C 178.5), from H-7 (δ_H 2.77) to C-11 (δ_C 178.5), from H_2-8 (δ_H 2.03-2.10, 1.65) to C-11 (δ_C 178.5), from H_3-14 (δ_H 1.00) to C-1 (δ_C 33.0), C-5 (δ_C 65.3), C-9 (δ_C 73.3) and C-10 (δ_C 47.1), from H_3-15 (δ_H 2.23) to C-4 (δ_C 213.2) and C-5 (δ_C 65.3), from H-3 (δ_H 4.38) to C-5 (δ_C 65.3) and C-6 (δ_C 27.7), along with the ^{1}H–^{1}H COSY correlations (Fig. 2) of H_2-6/H-7/H_2-8/H-9 and H_2-1/H_2-2/H-3, suggested a planar structure of 3-hydroxy-9-acetoxycyper-12,13-dinor-4-one-11-oic acid, representing a novel skeleton formed by the decarbonization of typical cyperane-type sesquiterpenes.

The relative configuration of **6** was determined through NOESY experiment analysis. NOESY correlations (Fig. 3) between H_3-14 and H_3-15 indicated a *cis*-junction between the two rings. The *α*-orientations of H-3, H-7, and H-9 were established by NOESY correlations (Fig. 3) observed between H-3/H-7, H-3/H-9, and H-7/H-9.

A biomimetic synthesis was conducted to verify the absolute configuration, also starting from the abundant compound **A** (Scheme 2). Compound **A** was initially protected through methyl esterification and subsequently subjected to oxidation using selenium dioxide, resulting in the formation of compound **6a** containing a hydroxy group at C-3. Treatment of compound **6a** with 4-methylbenzenesulfonhydrazide led to the formation of compound **6b**, which was then converted to the critical open-ring intermediate **6c** *via* ozonolysis [22]. Compound **6c** then underwent intramolecular aldol condensation, yielding compound **6d**. Following the final step of the biomimetic synthesis pathway of compound **1** (Scheme 1), compound **6** was successfully synthesized from **6d** using ruthenium(III) chloride and sodium periodate. Notably, no significant alterations in the stereochemistry of C-7, C-9, and C-10 were observed during the synthesis process.

TDDFT ECD calculations were also performed on the established structure of **6**. The high similarity between the calculated and experimental spectra further corroborated the proposed structure (Fig. 6). Consequently, the structure of compound **6** was conclusively determined to be (3*S*,5*R*,7*S*,9*S*,10*S*)-3-hydroxy-9-acetoxycyper-12,13-dinor-4-one-11-oic acid.

Compound **7** was assigned a molecular formula of $C_{17}H_{24}O_6$ based on HR-ESI-MS and ^{13}C NMR data (Table 3), indicating six degrees of unsaturation. The NMR data of **7** (Table 3) closely resembled those of **6**, with the exception of signals corresponding to an additional double bond (δ_H 6.38, 5.70; δ_C 143.3, 125.8), suggesting that compound **7** was a characteristic cyperane-type sesquiterpene. HMBC (Fig. 2) from H_3-2′ (δ_H 2.06) to C-1′ (δ_C 171.0), and from H-9 (δ_H 4.75) to C-1′ (δ_C 171.0) indicated an acetoxyl group attached to C-9. The planar structure of **7** was proposed as

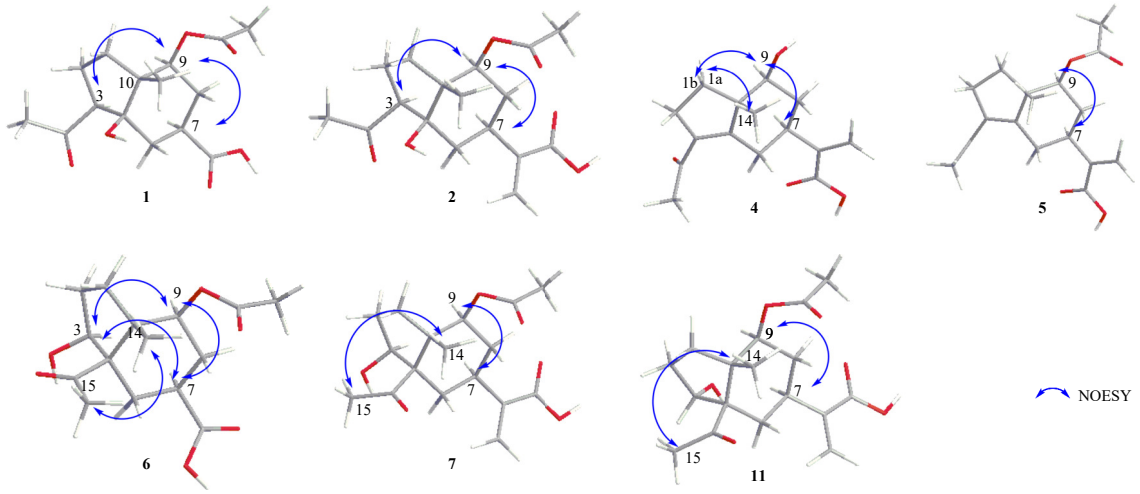

Fig. 3 Key NOESY correlations of compounds **1**, **2**, **4**–**6**, **7**, and **11**.

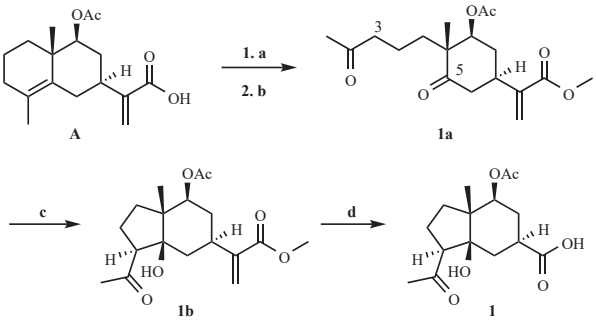

Scheme 1 Synthesis of compound **1** reagents and conditions: (a) $RuCl_3$, $NaIO_4$, DCM–Acetone–CH_3CN–H_2O, r.t., 1.5 h; (b) Me_2SO_4, K_2CO_3, Acetone, overnight, r.t.; (c) *t*-BuOK, THF, −78 °C, 3 h [20]; (d) $RuCl_3$, $NaIO_4$, DCM–Acetone–CH_3CN–H_2O, r.t., 2 h [21].

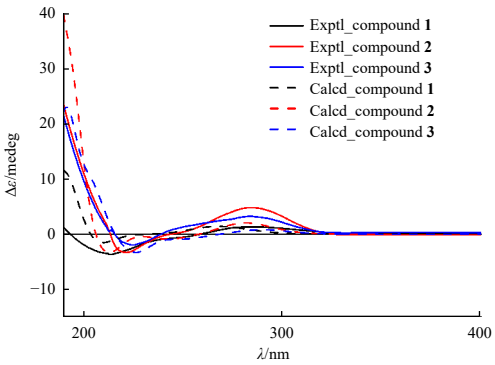

Fig. 4 Comparison of experimental and calculated ECD spectra of compounds **1**–**3** in MeOH.

3-hydroxy-9-acetoxycyper-11(13)-en-4-one-12-oic acid based on ^{1}H–^{1}H COSY and HMBC (Fig. 2). The NOESY spectrum of **7** (Fig. 3) exhibited identical correlations of H_3-14/H_3-15, H-3/H-7, H-7/H-9, and H-3/H-9 as observed in compound **6**, indicating an equivalent relative configuration. Considering compound **7** as a likely biosynthetic precursor of **6**, TDDFT ECD calculations were performed on the proposed structure, yielding a calculated spectrum highly consistent with the experimental data (Fig. 7). Consequently, the complete structure of **7** was elucidated as (3*S*,5*R*,7*S*,9*S*,10*S*)-3-hydroxy-9-acetoxycyper-11(13)-en-4-one-12-oic acid.

Compounds **8**–**10** were assigned identical molecular formulae of $C_{15}H_{22}O_5$, as determined by their HR-ESI-MS and ^{13}C NMR data (Table 4). Their NMR spectra (Table 4) closely resembled those of **7**, except for an absent acetoxyl group in these three compounds, indicating they might be deacetyl derivatives of **7**. The ^{1}H–^{1}H COSY and HMBC (Fig. 2) further corroborated that these compounds shared the same planar structure of 3,9-dihydroxycyper-11(13)-en-4-one-12-oic acid.

A comprehensive comparison of their NMR data revealed chemical shift differences at C-3, C-7, C-9, and C-14, suggesting that they might be diastereoisomers. Compound **8** exhibited identical NOESY correlations of H_3-14/H_3-15, H-3/H-7, and H-7/H-9, and a negative Cotton effect at 213 nm in the ECD spectrum, similar to compound **7** (Fig. 7), indicating they shared the same absolute configuration. The absolute configuration was further verified through a single-crystal X-ray crystallographic diffraction experiment using Cu Kα radiation (Fig. 8), as well as its calculated ECD spectrum (Fig. 7). Consequently, compound **8** was identified as (3*S*,5*R*,7*S*,9*S*,10*S*)-3,9-dihydroxycyper-11(13)-en-4-one-12-oic acid.

The primary distinction in ^{1}H NMR data between compounds **8** and **9** (Table 4) was observed in the coupling constant of H-3 (9.6, 7.1 Hz in **8** to 8.4, 3.9 Hz in **9**), suggesting an opposite orientation of OH-3. This structural elucidation was corroborated by a single-crystal X-ray diffraction analysis using Cu Kα radiation (Fig. 9), as well as its calculated ECD spectrum (Fig. 10). Consequently, the structure of **9** was determined to be (3*R*,5*R*,7*S*,9*S*,10*S*)-3,9-dihydroxycyper-11(13)-en-4-one-12-oic acid.

The NMR data of compound **10** indicated a naturally occurring cyperane-type sesquiterpene, sharing the same H-7α, H_3-14β, and H-9α configuration as compounds **8** and **9**, given their biogenesis, while differing at the C-3 or C-5 configuration. As the NOESY spectrum of **10** provided insufficient evidence, DFT NMR calculations were performed for four possible isomers (isomer 1, *3R*,*5R;* isomer 2, *3R*,*5S;* isomer 3, *3S*,*5R;* isomer 4, *3S*,*5S*). Conformation searching was conducted using Conflex 8.0 (Conflex Corporation, Tokyo, Japan, 2017) within an energy window of 5.0 kcal·mol^{-1}. Conformers with a Boltzmann distribution above 0.1% were selected for re-optimization at the M062X/6-31G(d) level *in vacuo*. Subsequently, NMR DFT calculations were performed on the re-optimized conformers at the M062X/6-311G(d, p) level with an SMD solvent model for acetone. The improved statistical method DP4+ was employed to analyze the calculated data of four possible isomers and the experimental data, yielding 100% for *3R*,*5S* (C, H, and all data, Supporting Fig. S89) [25, 26]. The established structure was utilized for TDDFT ECD calculation, and the calculated spectrum exhibited similar Cotton effects to the experimental one, confirming its absolute configuration (Fig. 10). Consequently, the complete structure of compound **10** was determined as (3*R*,5*S*,7*S*,9*S*,10*S*)-3,9-dihydroxycyper-11(13)-en-4-one-

Table 2 ^{1}H and ^{13}C NMR data for compounds **4** and **5** in $CDCl_3$.

No.	4		5	
	δ_H (J in Hz)[a]	δ_C[b]	δ_H (J in Hz)[a]	δ_C[c]
1	1.88, ddd (12.9, 8.1, 3.0) 1.82, dt (12.9, 9.3)	36.2, t	1.76[d]	35.9, t
2	2.68, m	31.8, t	2.66, m	31.8, t
3		134.3, s		134.8, s
4		199.6, s		199.3, s
5		158.4, s		156.9, s
6	3.42, ddd (14.0, 3.6, 1.7) 1.95[d]	29.4, t	3.44, dd (14.6, 4.0, 1.8) 2.03, ddt (14.6, 12.9, 3.1)	29.5, t
7	2.55, tt (12.9, 3.6)	37.0, d	2.62, tt (12.9, 3.1)	37.2, d
8	1.95[d] 1.82, dt (12.9, 9.3)	35.9, t	1.96 (d, 12.9) 1.76[d]	32.3, t
9	3.60, dd (12.9, 9.3)	78.4, d	4.79, dd (12.9, 4.4)	79.2, d
10		54.3, s		52.9, s
11		143.1, s		142.4, s
12		170.9, s		171.2, s
13	6.35, s 5.70, s	125.7, t	6.37, s 5.73, s	126.7, t
14	1.08, s	16.5, q	1.14, s	17.8, q
15	2.25, s	30.6, t	2.25, s	30.7, q
1′				170.7, s
2′			2.07, s	21.4, q

[a] measured at 600 MHz; [b] measured at 125 MHz; [c] measured at 100 MHz; [d] overlapped.

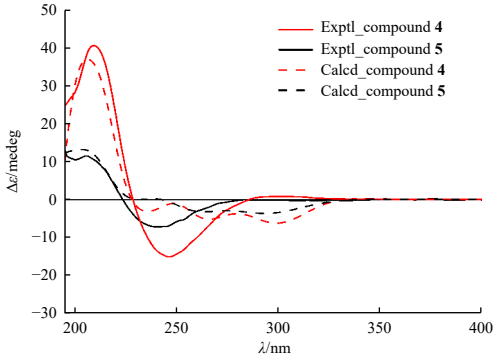

Fig. 5 Comparison of experimental and calculated ECD spectra of compounds **4** and **5** in MeOH.

12-oic acid.

The molecular formula of compound **11** was determined to be $C_{17}H_{24}O_6$ based on HR-ESI-MS and ^{13}C NMR data (Table 4). Comparison of NMR data (Table 4) of **9** and **11**, along with their respective molecular formulas, indicated the presence of an additional acetoxyl group in **11**. HMBC (Fig. 2) from H_3-2′ (δ_H 2.07) to C-1′ (δ_C 171.2), and from H-9 (δ_H 5.18) to C-1′ (δ_C 171.2) confirmed that the acetoxyl group was attached to C-9. Considering its biogenesis, compound **11** was proposed to be a C-9 acetyl derivative of **9**. The calculated ECD spectrum of the proposed structure of **11** corresponded well with the experimental ECD spectrum (Fig. 10), supporting the same absolute configuration. Consequently, compound **11** was identified as (3*R*,5*R*,7*S*,9*S*,10*S*)-3-hydroxy-9-acetoxycyper-11(13)-en-4-one-12-oic acid.

Table 3 ^{1}H and ^{13}C NMR data for compounds **6** and **7** in $CDCl_3$.

No.	6		7	
	δ_H (J in Hz)[a]	δ_C[b]	δ_H (J in Hz)[c]	δ_C[d]
1	1.74, td (12.5, 7.0) 1.52, ddd (12.5, 9.4, 2.5)	33.0, t	1.80[e] 1.57[e]	33.3, t
2	2.29–2.40[e] 1.82, tdd (13.6, 6.6, 2.5)	31.2, t	2.37, m 1.80[e]	31.3, t
3	4.38, dd (10.1, 6.6)	76.1, d	4.59, dd (10.1, 6.0)	76.2, d
4		213.2, s		213.4, s
5		65.3, s		65.9, s
6	2.99–2.40[e] 2.03–2.10[e]	27.7, t	2.23, br d (13.3) 1.80[e]	31.9, t
7	2.77, tt (12.9, 3.7)	37.4, d	2.94, t (12.7)	33.2, d
8	2.03–2.10[e] 1.65, q (12.4)	29.1, t	1.80[e] 1.57[e]	31.7, t
9	4.63, dd (12.4, 4.0)	73.3, d	4.75, dd (12.1, 3.9)	74.6, d
10		47.1, s		47.3, s
11		178.5, s		143.3, s[f]
12				169.9, s[f]
13			6.38, s 5.70, s	125.8, t
14	1.00, s	15.6, q	1.00, s	15.7, q
15	2.23, s	31.9, q	2.20, s	31.9, q
1′		171.0, s		171.0, s
2′	2.08, s	21.3, q	2.06, s	21.3, q

[a] measured at 600 MHz; [b] measured at 150 MHz; [c] measured at 500 MHz; [d] measured at 125 MHz; [e] overlapped; [f] signals identified from HMBC spectrum.

All isolates were evaluated for their anti-hepatic fibrosis activities by assessing the RNA expression of *α-SMA* in human HSCs induced by TGF-β [27]. The results indicated that compounds **2**, **6**, **8**, and **10** significantly reduced the expression of *α-SMA* mRNA (Fig. 11). Moreover, the study identified correlations between the substitution pattern of the iphionane-type or cyperane-type sesquiterpenes and their anti-hepatic fibrosis activity. The iphionane-type sesquiterpene derivatives with a 9-acetoxyl group (**2** and **4**) demonstrated higher potency compared to those with a 9-hydroxy group (**3** and **5**). However, for cyperane-type sesquiterpenes, an acetoxyl group at C-9 appeared unfavorable, as compounds **10** and **12** exhibited higher activity than the 9-acetoxyl derivatives compounds **7** and **8**. Furthermore, the comparison of compounds **7**–**11**, which shared the same skeleton, suggested that cyperane-type sesquiterpenes with the same orientations as *α* (**10**) or *β* (**7** and **8**) were more potent than those with the opposite orientations (**9** and **11**). These findings underscore the need for further research to establish more comprehensive structure-activity relationships in the context of anti-hepatic fibrosis activities.

In conclusion, the phytochemical investigation of *A. hedinii* resulted in the isolation and structural elucidation of 11 novel sesquiterpenoids, comprising four iphionane-types, five cyperane-types, and two previously unidentified skeleton types. Notably, two sesquiterpenoids with new skeletons were successfully synthesized using biomimetic methods, overcoming the challenges

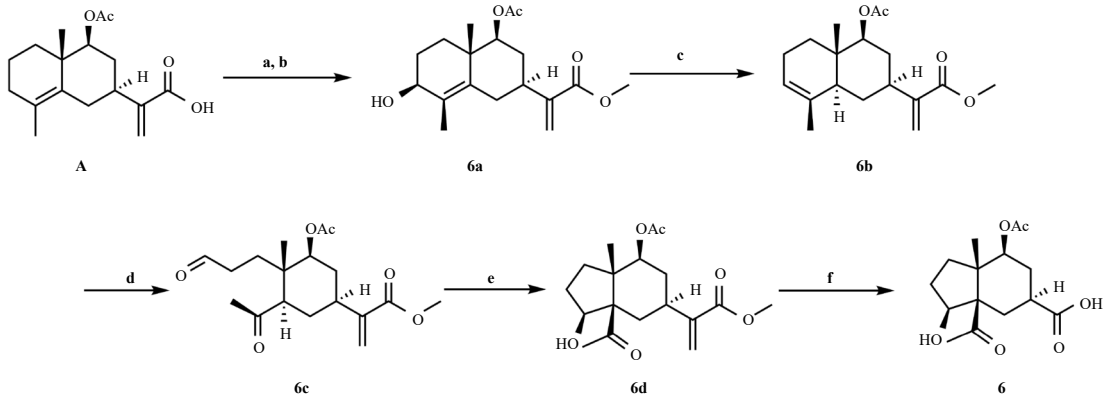

Scheme 2 Synthesis of compound **6** reagents and conditions: (a) Me_2SO_4, K_2CO_3, Acetone, overnight, r.t.; (b) SeO_2, *t*-BuOOH, DCM [23]; (c) $TsNHNH_2$, CH_3CN, 90 °C [22]; (d) O_3, Pyr, DCM, −78 °C [24]; (e) *t*-BuOK, THF, −78 °C, 2 h [20]; (f) $RuCl_3$, $NaIO_4$, DCM–Acetone–CH_3CN–H_2O, r.t., 2 h [21].

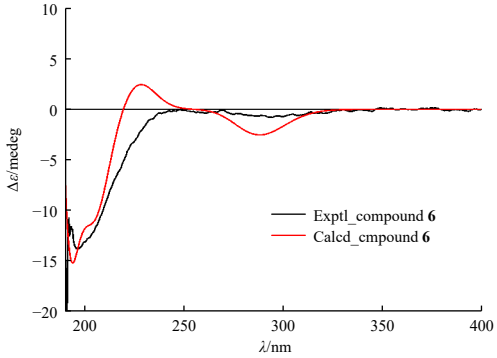

Fig. 6 Comparison of experimental and calculated ECD spectra of compound **6** in MeOH.

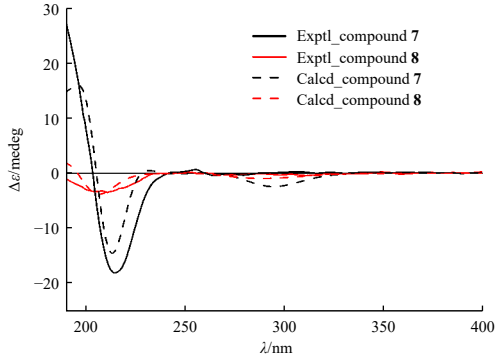

Fig. 7 Comparison of experimental and calculated ECD spectra of compounds **7** in MeOH and **8** in CH_3CN.

associated with limited compound content and stereoscopic configuration. Moreover, compounds **2**, **8**, and **10** exhibited significant inhibitory effects on the mRNA expression of *α-SMA*, suggesting their potential in the treatment of hepatic fibrosis. Additionally, this study provides a preliminary analysis of the correlations between substitution patterns of iphionane-type or cyperane-type sesquiterpenes and their anti-hepatic fibrosis activity, enhancing our understanding of the structure-activity relationship in this context.

3. Experimental

3.1. General experimental procedures

NMR spectra were acquired using Bruker AVANCE III instruments operating at 400, 500, 600, or 800 MHz (Bruker Biospin AG, Switzerland). HR-ESI-MS data were obtained on Waters Synapt G2-Si Q-Tof mass spectrometers (Waters, USA). LC-ESI-MS data were collected using a Waters 2695 instrument equipped with a 2998 PDA detector, a Waters Acquity ELSD 2424, and a Waters 3100 SQDMS detector (Waters, USA). Preparative high-performance liquid chromatography (HPLC) was performed on a Waters 2545 Binary Gradient Module instrument with a Waters 2489 UV/visible detector, utilizing a SunFire column (Prep C_{18} OBD, 5 μm, 30 mm × 150 mm, Waters, Ireland). Column chromatography was conducted using MCI gel CHP20P (75–150 μm, Mitsubishi Chemical Industries, Tokyo, Japan), silica gel (100–200, 200–300, and 300–400 mesh, Qingdao Marine Chemical Industrials, Qingdao, China), ODS gel AAG12S50 (12 nm, S-50 μm, YMC, Japan), Sephadex LH-20 (Pharmacia Biotech AB, Uppsala, Sweden), Toyopearl HW-40F (Tosoh Corporation, Tokyo, Japan), and DIOL MB100-75/200 (Fuji Silysia, Aichi-Ken, Japan). Thin layer chromatography (TLC) was performed on precoated silica gel GF_{254} plates (Yantai Chemical Industrials, Yantai, China) and HPTLC silica gel 60 DIOL F254s (Merck KGaA, Darmstadt, German). TLC spots were visualized at 254 nm and with 5% H_2SO_4 in EtOH containing 10 mg·mL^{-1} vanillin by heating. Solvents for column chromatography were of analytical grade (Shanghai Chemical Reagents Co., Ltd., Shanghai, China), while those for analytic and preparative HPLC were of HPLC grade (Merck KGaA, Darmstadt, Germany; Ourchem, Shanghai, China). Reagents and solvents were used without further purification. Optical rotation values were measured on a Rudolph Research Analytical Autopol VI 90079 polarimeter (Hackettstown, NJ, USA). IR spectra were recorded using a Thermo Nicolet FTIR IS5 spectrometer with KBr disks (ThermoFisher, USA). Single-crystal X-ray diffraction measurements were conducted using a Bruker D8 Venture diffractometer or a Bruker Apex-II CCD diffractometer (Bruker, Germany).

3.2. Plant material

The entire plants of *A. hedinii* were harvested from Ganzi Prefecture, Sichuan Province, China, in November 2018. Jun Zhang from Kunming Zhifen Biotechnology Co., Ltd. (Kunming, China) authenticated the species. A voucher specimen (No. 20181124) was deposited at the Herbarium of the Shanghai Institute of Materia Medica, Chinese Academy of Sciences.

3.3. Extraction and isolation

The entire *A. Hedinii* plant (50 kg) underwent extraction with 95% EtOH at room temperature three times [15]. The combined percolates were evaporated under pressure, yielding a crude residue (3.5 kg). This residue was suspended in water and successively extracted with petroleum ether (PE) and CH_2Cl_2, produ-

Table 4 ^{1}H and ^{13}C NMR data for compounds **9**–**11**.

No.	**8**[a]		**9**[b]		**10**[a]		**11**[c]	
	δ_H (J in Hz)[d]	δ_C[e]	δ_H (J in Hz)[d]	δ_C[e]	δ_H (J in Hz)[d]	δ_C[e]	δ_H (J in Hz)[d]	δ_C[f]
1	2.01, m 1.84, m	34.3, t 1.84, m	1.69, m 1.41, m	33.5, t	2.56, dt (12.2, 5.9) 1.30, ddd (11.7, 9.5, 3.7)	32.6, t	1.76–1.85[g] 1.54, dt (13.2, 10.1)	33.0, t
2	2.22, m 2.05[g]	31.4, t 2.05[g]	2.22, m	34.1, t	2.17, m 1.41, tdd (12.2, 7.7, 3.7)	31.3, t	2.38, dddd (14.5, 10.1, 8.3, 1.6) 1.76–1.85[g]	33.5, t
3	4.57, dd (9.6, 7.1)	76.1, d	4.30, dd (8.4, 3.9)	79.2, d	4.34, t (8.2)	77.8, d	4.45, dd (8.3, 3.8)	79.1, d
4		212.0, s		214.0, s		213.0, s		212.4, s
5		66.2, s		66.6, s		65.7, s		66.1, s
6	2.12, dt (13.8, 2.6) 1.84, m	32.1, t 1.84, m	1.88, dd (13.8, 12.6)	32.4, t	2.40, dd (13.7, 3.7) 1.67, tdd (12.2, 7.7, 3.7)	33.2, t	2.23, dd (12.9, 2.6) 1.68, dd (12.9, 8.9)	32.4, t
7	2.85, t (12.3)	33.8, d	3.32, tt (12.6, 4.0)	35.4, d	2.48, tt (12.2, 3.7)	37.2, d	3.48, tt (12.9, 3.9)	34.4, d
8	1.75, d (12.3) 1.41, q (12.3)	36.9, t 1.41, q (12.3)	1.68, m 1.41, m	35.3, t	1.67, m 1.58, q (12.2)	36.1, t	1.76–1.85[g] 1.62, q (12.0)	30.5, t
9	3.47, dd (12.3, 3.8)	73.3, d	3.76, ddd (11.8, 3.8, 1.3)	71.5, d	4.14, dd (11.0, 4.9)	70.3, d	5.18, dd (12.0, 3.7)	74.2, d
10		49.1, s		49.9, s		50.6, s		48.1, s
11		146.3, s		146.6, s		145.9, s		144.3, s
12		168.6, s		169.1, s		168.7, s		171.1, s[h]
13	6.24, s 5.76, s	123.4, t 5.76, s	6.15, s 5.68, s	123.7, t	6.22, s 5.73, s	123.5, t	6.33, s 5.66, s	125.4, t
14	0.88, s	14.3, q	0.87, s	15.1, q	0.95, s	18.4, q	1.02, s	15.9, q
15	2.17, s	32.0, q	2.12, s	30.5, q	2.31, s	32.2, q	2.16, s	30.3, q
1′								171.2, s[h]
2′							2.07, s	21.4, q

[a] Acetone-d_6; [b] Acetonitrile-d_3; [c] $CDCl_3$; [d] measured at 600 MHz; [e] measured at 125 MHz; [f] measured at 100 MHz; [g] overlapped; [h] signals identified from HMBC spectrum.

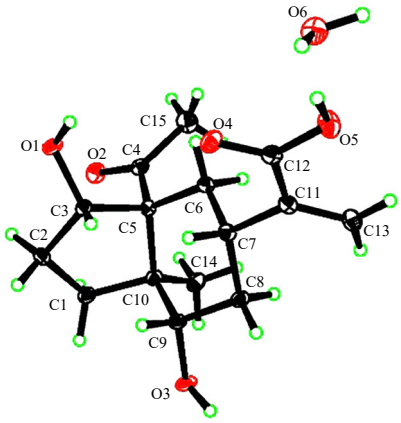

Fig. 8 ORTEP drawing of compound **8**.

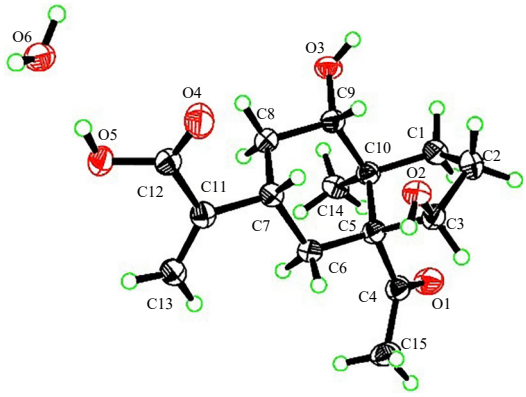

Fig. 9 ORTEP drawing of compound **9**.

cing PE (2.6 kg) and CH_2Cl_2 (1.7 kg) fractions. The CH_2Cl_2 fraction underwent chromatographic separation on an MCI column, eluted with an aqueous EtOH gradient (40%, 60%, 80%, and 95%), resulting in four fractions (Frs. 1–4). Fr. 1 (207 g) was chromatographed over an MCI column, eluted with aqueous MeOH (30%, 40%, 50%, 60%, 70%, 80%, and 90%), yielding 11 fractions (Frs. 1A–1K). Frs.1A–1C were subjected to an ODS gel column elution with an aqueous MeOH gradient, producing subfractions Frs. 1A1–1A7, Frs. 1B1–1B8, and Frs. 1C1–1C9. Fr. 1A1 (1.3 g) underwent separation using a silica gel column (300–400 mesh) eluted with CH_2Cl_2/MeOH (20∶1, 10∶1), affording compounds **1** (125 mg), **4** (18 mg), and **6** (14 mg). Fr. 1B5 (4.64 g) and Fr. 1C4 (6.72 g) were subjected to silica gel CC (300–400 mesh) with isocratic elution of $CHCl_3$/MeOH (50∶1), followed by a silica gel column (300–400 mesh) eluted with CH_2Cl_2/MeOH (20∶1), yielding compounds **2** (25 mg) and **3** (5 mg). Fr. 1B7 (2.2 g) underwent separation using a silica gel column (300–400 mesh) eluted with PE/EtOAc (6∶1, 5∶1, 4∶1), producing compound **5** (949 mg). Fr. 1C5 (2.7 g) and Fr. 1C7 (1.6 g) were separated by CC on Sephadex LH-20 gel (eluted with MeOH) and then silica gel (300–400 mesh, PE/EtOAc, 10∶1–1∶1), yielding compounds **7** (721 mg) and **11** (60 mg). Fr. 2 (204 g) was chromatographed over an MCI column with aqueous EtOH (30%, 35%, 40%, 45%, 50%, 55%, and 95%), resulting in 18 fractions (Frs. 2A–2R). Compound **9** (10 mg) was obtained from the PE fraction (2.6 kg) by CC over an ODS gel column with aqueous MeOH gradient elution and repeated DIOL silica gel columns (100–75/200 mesh, CH_2Cl_2/MeOH, 20∶1; PE/EtOAc, 5∶1–1∶1). Compounds **8** (75 mg) and **10** (3 mg) were obtained from DIOL silica gel

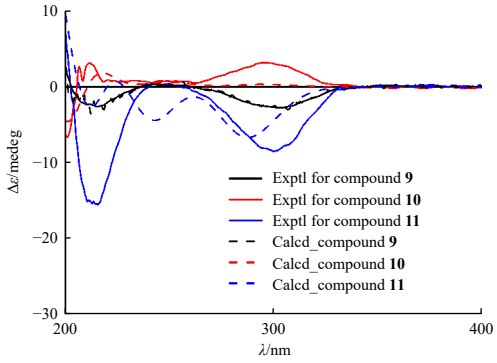

Fig. 10 Comparison of experimental and calculated ECD spectra of compounds **9** and **10** in CH_3CN and **11** in MeOH.

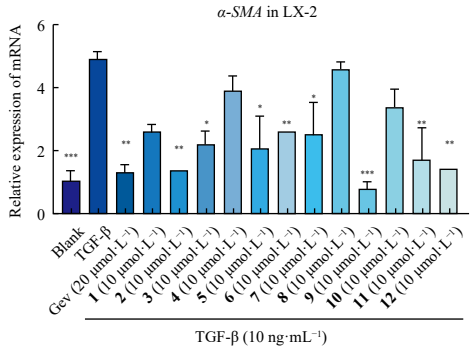

Fig. 11 The relative content of *α-SMA* mRNA in LX-2. The mRNA relative content of the *α-SMA* gene in LX-2 after treatment with 10 μmol·L^{-1} of compounds or positive control for 12 h under stimulated conditions and control with or without stimulation and their mRNA relative content were determined. Data are represented as mean ± SD of three independent experiments. $^{*}P < 0.05$, $^{**}P < 0.01$, $^{***}P < 0.001$ *vs* stimulated control group, in multivariate analysis using one-way ANOVA.

columns (100–75/200 mesh) eluted with PE/EtOAc (2∶1) and preparative HPLC (MeCN/H_2O, 0–35 min, from 10%–30% and 15%–35%, respectively).

(3*S*,5*S*,7*R*,9*S*,10*R*)-5-hydroxy-9-acetoxyiphion-12,13-dinor-4-one-11-oic acid (**1**): colorless oil; $[\alpha]_D^{20}$ +32 (*c* 0.1, MeOH); UV (MeOH) (log *ε*) 203 (1.93) nm; ECD (MeOH) λ_{max} (Δ*ε*) 217 (−9.37) nm, 284 (+12.74) nm; IR (KBr) ν_{max} 3445, 2922, 1731, 1714, 1367, 1245, 1182 cm^{-1}; ^1H and ^{13}C NMR data see Table 1; HR-ESI-MS *m/z* 297.1332 $[M - H]^-$ (Calcd. for $C_{15}H_{21}O_6$, 297.1338).

(3*S*,5*S*,7*R*,9*S*,10*R*)-5-hydroxy-9-acetoxyiphio-4-one-11(13)-en-12-oic acid (**2**): colorless oil; $[\alpha]_D^{20}$ +71 (*c* 0.1, MeOH); UV (MeOH) (log *ε*) 203 (2.89) nm; ECD (MeOH) λ_{max} (Δ*ε*) 196 (+11.77) nm, 218 (−13.09) nm, 284 (+17.05) nm; IR (KBr) ν_{max} 3346, 2947, 1714, 1384, 1244, 1181 cm^{-1}; ^1H and ^{13}C NMR data see Table 1; HR-ESI-MS *m/z* 323.1496 $[M - H]^-$ (Calcd. for $C_{17}H_{23}O_6$, 323.1495).

(3*S*,5*S*,7*R*,9*S*,10*R*)-5,9-dihydroxyiphio-4-one-11(13)-en-12-oic acid (**3**): colorless oil; $[\alpha]_D^{20}$ +71 (*c* 0.1, MeOH); UV (MeOH) (log *ε*) 205 (2.29) nm; ECD (MeOH) λ_{max} (Δ*ε*) 191 (+8.52) nm, 220 (−9.82) nm, 285 (+12.72) nm; IR (KBr) ν_{max} 3444, 2943, 1704, 1698, 1374, 1243, 1180 cm^{-1}; ^1H and ^{13}C NMR data see Table 1; HR-ESI-MS *m/z* 281.1394 $[M - H]^-$ (Calcd. for $C_{15}H_{21}O_5$, 281.1389).

(7*S*,9*S*,10*S*)-9-hydroxyiphio-3(5),11(13)-dien-4-one-12-oic acid (**4**): colorless oil; $[\alpha]_D^{20}$ +43 (*c* 0.1, MeOH); UV (MeOH) (log *ε*) 255 (3.78) nm; ECD (MeOH) λ_{max} (Δ*ε*) 210 (+5.91) nm, 249 (−7.01) nm; IR (KBr) ν_{max} 3440, 2935, 1704, 1622, 1418, 1362, 1271 cm^{-1}; ^1H and ^{13}C NMR data see Table 2; HR-ESI-MS *m/z* 263.1283 $[M - H]^-$ (Calcd. for $C_{15}H_{19}O_4$, 263.1283).

(7*S*,9*S*,10*S*)-9-acetoxyiphio-3(5),11(13)-dien-4-one-12-oic acid (**5**): colorless oil; $[\alpha]_D^{20}$ +82 (*c* 0.1, MeOH); UV (MeOH) (log *ε*) 251 (1.74) nm; ECD (MeOH) λ_{max} (Δ*ε*) 204 (+14.47) nm, 239 (−16.96) nm; IR (KBr) ν_{max} 3212, 2936, 1716, 1682, 1622, 1362, 1238, 1155 cm^{-1}; ^1H and ^{13}C NMR data see Table 2; HR-ESI-MS *m/z* 305.1390 $[M - H]^-$ (Calcd. for $C_{17}H_{21}O_5$, 305.1389).

(3*S*,5*R*,7*S*,9*S*,10*S*)-3-hydroxy-9-acetoxycyper-12,13-dinor-4-one-11-oic acid (**6**): colorless oil; $[\alpha]_D^{20}$ +85 (*c* 0.1, MeOH); UV (MeOH) (log *ε*) 205 (3.35) nm; ECD (MeOH) λ_{max} (Δ*ε*) 201 (−7.51) nm; IR (KBr) ν_{max} 3445, 2949, 1715, 1417, 1373, 1242 cm^{-1}; ^1H and ^{13}C NMR data see Table 3; HR-ESI-MS *m/z* 297.1341 $[M - H]^-$ (Calcd. for $C_{17}H_{23}O_6$, 297.1338).

(3*S*,5*R*,7*S*,9*S*,10*S*)-3-hydroxy-9-acetoxycyper-11(13)-en-4-one-12-oic acid (**7**): colorless oil; $[\alpha]_D^{20}$ +93 (*c* 0.1, MeOH); UV (MeOH) (log *ε*) 203 (3.08) nm; ECD (MeOH) λ_{max} (Δ*ε*) 216 (−9.41) nm; IR (KBr) ν_{max} 3444, 2946, 1698, 1423, 1374, 1243 cm^{-1}; ^1H and ^{13}C NMR data see Table 3; HR-ESI-MS *m/z* 323.1512 $[M - H]^-$ (Calcd. for $C_{17}H_{23}O_6$, 323.1495).

(3*S*,5*R*,7*S*,9*S*,10*S*)-3,9-dihydroxycyper-11(13)-en-4-one-12-oic acid (**8**): colorless block-shaped crystals; $[\alpha]_D^{20}$ +30 (*c* 0.1, CH_3CN); UV (Acetone) (log *ε*) 207 (5.63) nm; ECD (CH_3CN) λ_{max} (Δ*ε*) 213 (−12.37) nm; IR (KBr) ν_{max} 3398, 2959, 2917, 1689, 1465, 1375, 1217, 1181 cm^{-1}; ^1H and ^{13}C NMR data see Table 4; HR-ESI-MS *m/z* 281.1373 $[M - H]^-$ (Calcd. for $C_{15}H_{21}O_5$, 281.1389).

(3*R*,5*R*,7*S*,9*S*,10*S*)-3,9-dihydroxycyper-11(13)-en-4-one-12-oic acid (**9**): colorless block-shaped crystals; $[\alpha]_D^{20}$ +11 (*c* 0.1, CH_3CN); UV (MeCN) (log *ε*) 198 (2.10) nm; ECD (CH_3CN) λ_{max} (Δ*ε*) 245 (+13.27) nm, 296 (−16.01) nm; IR (KBr) ν_{max} 3414, 2919, 1706, 1687, 1423, 1353, 1242 cm^{-1}; ^1H and ^{13}C NMR data see Table 4; HR-ESI-MS *m/z* 281.1383 $[M - H]^-$ (Calcd. for $C_{15}H_{21}O_5$, 281.1389).

(3*R*,5*S*,7*S*,9*S*,10*S*)-3,9-dihydroxycyper-11(13)-en-4-one-12-oic acid (**10**): colorless oil; $[\alpha]_D^{20}$ +19 (*c* 0.1, CH_3CN); UV (MeCN) (log *ε*) 199 (3.08) nm; ECD (CH_3CN) λ_{max} (Δ*ε*) 297.5 (+9.44) nm; IR (KBr) ν_{max} 3381, 2927, 2854, 1735, 1716, 1467, 1271 cm^{-1}; ^1H and ^{13}C NMR data see Table 4; HR-ESI-MS *m/z* 281.1385 $[M - H]^-$ (Calcd. for $C_{15}H_{21}O_5$, 281.1389).

(3*R*,5*R*,7*S*,9*S*,10*S*)-3-hydroxy-9-acetoxycyper-11(13)-en-4-one-12-oic acid (**11**): colorless oil; $[\alpha]_D^{20}$ +15 (*c* 0.1, MeOH); UV (MeOH) (log *ε*) 203 (1.62) nm; ECD (MeOH) λ_{max} (Δ*ε*) 212 (−7.94) nm, 301 (−11.27) nm; IR (KBr) ν_{max} 3445, 2949, 1714, 1692, 1373, 1246 cm^{-1}; ^1H and ^{13}C NMR data see Table 4; HR-ESI-MS *m/z* 323.1492 $[M - H]^-$ (Calcd. for $C_{17}H_{23}O_6$, 323.1495).

*3.4. X-ray crystallographic analysis of compounds **8** and **9***

Crystals were obtained from their respective CH_3CN solutions. Suitable specimens were selected for X-ray crystallographic analysis. The structure was solved and refined using the Bruker Shelxtl software package. Crystallographic data for each crystal can be accessed free of charge *via* the internet at www.ccdc.cam.ac.uk/conts/retrieving.html or by application to the Cambridge Crystallographic Data Centre (CCDC), 12 Union Road, Cambridge CB2 1EZ, UK [Tel.: (+44)-1223-336-408; Fax: (+44)-1223-336-033; E-mail: deposit@ccdc.cam.ac.uk].

Crystal data for compound **8**: the crystal was maintained at 140 K during data collection. $C_{15}H_{24}O_6$ (*Mr* = 300.34 g·mol^{-1}): monoclinic, space group $P2_1$ (No. 4), *a* = 7.0927 (3) Å, *b* = 15.6810 (6) Å, *c* = 7.6235 (3) Å, *α* = 90°, *β* = 117.0350 (10)°, *γ* = 90°, *V* = 755.24 (5) $Å^3$, *Z* = 2, *T* = 170 K, *μ*(Cu K*α*) = 0.844 mm^{-1}, D_{calc} = 1.321 g·cm^{-3}, 7293 reflections measured (15.118° ≤ 2*σ* ≤ 148.708°), 2873 unique [R_{int} = 0.0523, R_{sigma} = 0.0595] which were utilized in all calculations. The final R_1 was 0.0386 ($I > 2\sigma(I)$], and wR_2 was 0.1018 (all data). Flack parameter: 0.02 (8). Crystallographic data for **12** have been deposited at CCDC under deposit No. CCDC2341997.

Crystal data for compound **9**: The crystal was maintained at 140 K during data collection. $C_{15}H_{24}O_6$ (*Mr* = 300.34 g·mol^{-1}): orthorhombic, space group $P2_12_12_1$ (No. 19), *a* = 10.0013 (4) Å, *b* =

10.0117 (8) Å, c = 14.9562 (12) Å, α = 90°, β = 90°, γ = 90°, V = 1497.56 (18) Å^3, Z = 4, T = 100 K, μ(Cu Kα) = 0.852 mm^{-1}, D_{calc} = 1.332 g·cm^{-3}, 16 744 reflections measured (10.634° ≤ 2σ ≤ 143.934°), 2917 unique (R_{int} = 0.0639, R_{sigma} = 0.0442) which were utilized in all calculations. The final R_1 was 0.0431 [I > 2σ(I)] and wR_2 was 0.1127 (all data). Flack parameter: 0.10 (7). Crystallographic data for **9** have been deposited at the CCDC under deposit No. CCDC2341996.

3.5. LX-2 cell culture and treatment

The human LX-2 HSCs were obtained from the Cell Bank, Chinese Academy of Sciences (Shanghai, China). LX-2 cells were cultivated in Dulbecco's modified eagle medium (DMEM) (HyClone, Logan, UT) supplemented with penicillin (100 U·mL^{-1}), streptomycin (100 mg·mL^{-1}), and 10% fetal bovine serum (Gibco, Carlsbad, CA). Prior to the experiment, LX-2 cells were seeded into twelve-well plates for 12 h. In this study, LX-2 cells were maintained in a serum-free medium for 24 h and subsequently treated with compounds and 10 ng·mL^{-1} TGF-β (PeproTech) for an additional 24 h [27].

3.6. Real-time quantitative polymerase chain reaction (RT-qPCR)

Total RNA was extracted from cells using TRIzol reagent (Life Technology, CA) and purified with EZ-10 spin columns and collection tubes (Sangon Biotech, Shanghai, China). The RNA was reverse-transcribed to complementary deoxyribonucleic acid (cDNA) utilizing PrimeScript RT Master Mix as per the manufacturer's instructions (Yeasen Biotech Co., Ltd., Shanghai, China). The cDNA was then diluted and combined with primers and Hieff qPCR SYBR Green Master Mix (Yeasen Biotech Co., Ltd.). RT-qPCR was conducted using the Applied Biosystems 7500 Fast Real-Time PCR system (Thermo Fisher Scientific). The results were normalized to glyceraldehyde-3-phosphate dehydrogenase (GAPDH) and analyzed using the delta-delta C_t method. The primers for the genes are detailed in Table S1 in Supporting information.

Funding

This work was supported from the National Natural Science Foundation of China (No. 21920102003), the Key-Area Research and Development Program of Guangdong Province (No. 2020B0303070002), and the National Key R&D Program "Strategic Scientific and Technological Innovation Cooperation" Key Project (No. 2022YFE0203600).

Declaration of competing interest

These authors have no conflict of interest to declare.

Availability of supporting information

Determination of absolute configuration of compound **A**; experimental procedures of biomimetic synthesis; 1D and 2D NMR data, IR spectra, and HR-ESI-MS of isolated new compounds (**1**–**11**) and 1D NMR data of key intermediate compounds (**1a**, **1b**, **1**, **6a**–**6d**, **6**); DFT NMR calculations of compound **10**; Primers for Real-Time PCR. All of these supporting information can be requested by sending E-mail to the corresponding author.

References

1 Martin VJJ, Pitera DJ, Withers ST, et al. Engineering a mevalonate pathway in *Escherichia coli* for production of terpenoids. *Nat Biotechnol*. 2003;21:796-802. https://doi.org/10.1038/nbt833.
2 El-Ghazouly MG, El-Sebakhy NA, El-Din AAS, et al. Sesquiterpene xylosides from *Iphiona scabra*. *Phytochemistry*. 1987;26(2):439-443. https://doi.org/10.1016/S0031-9422(00)81428-4.
3 Ahmed AA, Mahmoud AA. Jasonol, a rare tricyclic eudesmane sesquiterpene and six other new sesquiterpenoids from *Jasonia candicans*. *Tetrahedron*. 1998;54(28):8141-8152. https://doi.org/10.1016/S0040-4020(98)00453-0.
4 Todorova MN, Evstatieva LN. Comparative study of tanacetum species growing in Bulgaria. *Z Naturforsch C J Biosci*. 2001;56(7-8):506-512. https://doi.org/10.1515/znc-2001-7-806.
5 Tian LW, Xu M, Li XC, et al. Eucalmaidials A and B, phloroglucinol-coupled sesquiterpenoids from the juvenile leaves of *Eucalyptus maideni*. *RSC Adv*. 2014;4(41):21373-21378. https://doi.org/10.1039/C4RA01078G.
6 Wu HB, Ma LH, Li XM, et al. Selective phytotoxic effects of sesquiterpenoids from *Sonchus arvensis* as a preliminary approach for the biocontrol of two problematic weeds of wheat. *J Agric Food Chem*. 2022;70(30):9412-9420. https://doi.org/10.1021/acs.jafc.2c03462.
7 Hikino H, Aota K, Maebayashi Y, et al. Structure and absolute configuration of cyperolone. *Chem Pharm Bull*. 1967;15(9):1349-1355. https://doi.org/10.1248/cpb.15.1349.
8 Hikino H, Hikino Y, Agatsuma K, et al. Structure and absolute configuration of faurinone. *Chem Pharm Bull*. 1968;16(9):1779-1783. https://doi.org/10.1248/cpb.16.1779.
9 Ahmed AA, Jakupovic J. Sesqui- and monoterpenes from *Jasonia montana*. *Phytochemistry*. 1990;29(11):3658-3661. https://doi.org/10.1016/0031-9422(90)85296-R.
10 Ohira S, Hasegawa T, Hayashi KI, et al. Sesquiterpenoids from *Cyperus rotundus*. *Phytochemistry*. 1998;47(8):1577-1581. https://doi.org/10.1016/S0031-9422(97)00825-X.
11 Todorova MN, Tsankova ET. New sesquiterpenoids from *Achillea clypeolata*. *Phytochemistry*. 1999;52(8):1515-1518. https://doi.org/10.1016/S0031-9422(99)00350-7.
12 Baser KHC, Demirci B, Iscan G, et al. The essential oil constituents and antimicrobial activity of *Anthemis aciphylla* BOISS. var. *discoidea* BOISS. *Chem Pharm Bull*. 2006;54(2):222-225. https://doi.org/10.1248/cpb.54.222.
13 Ceccherelli P, Curini M, Marcotullio MC, et al. Biogenetic-type transformation of 3-keto-4,5-epoxy-eudesmanes: synthesis of cyperanes, eremophilanes and spirovetivanes. *Tetrahedron*. 1989;45(12):3809-3818. https://doi.org/10.1016/S0040-4020(01)89241-3.
14 Bora KS, Sharma A. The genus Artemisia: a comprehensive review. *Pharm Biol*. 2010;49(1):101-109. https://doi.org/10.3109/13880209.2010.497815.
15 Wang X, Peng X, Tang C, et al. Anti-inflammatory eudesmane sesquiterpenoids from *Artemisia hedinii*. *J Nat Prod*. 2021;84(5):1626-1637. https://doi.org/10.1021/acs.jnatprod.1c00177.
16 Wang X, Tang C, Meng S, et al. Noreudesmane sesquiterpenoids from *Artemisia hedinii* and their anti-inflammatory activities. *Fitoterapia*. 2021;153:104961. https://doi.org/10.1016/j.fitote.2021.104961.
17 Si C. *Study on the Pharmacodynamic Material Basis of Tibetan Medicine Artemisia hedinii Ostenf. et Pauls. Against Intrahepatic Cholestatic Liver Injury and Its Quality Standard*. Jiangxi University of Traditional Chinese Medicine, Nanchang, 2023.
18 Tao L, Yang G, Sun T, et al. Capsaicin receptor TRPV1 maintains quiescence of hepatic stellate cells in the liver *via* recruitment of SARM1. *J Hepatol*. 2023;78(4):805-819. https://doi.org/10.1016/j.jhep.2022.12.031.
19 Rustaiyan A, Bamonieri A, Raffatrad M, et al. Eudesmane derivatives and highly oxygenated monoterpenes from Iranian *Artemisia* species. *Phytochemistry*. 1987;26(8):2307-2310. https://doi.org/10.1016/S0031-9422(00)84708-1.
20 Gao XL, Xiong ZM, Zhou G, et al. First enantioselective total synthesis and absolute configurations of 4,5-dioxo-seco-γ-eudesmol and 5β,11-dihydroxyiphionan-4-one, two aglycones of naturally occurring sesquiterpenes with new skeletons. *Synthesis*. 2001;1:37-39. https://doi.org/10.1055/s-2001-9742.
21 Buskas T, Söderberg E, Konradsson P, et al. Use of *n*-pentenyl glycosides as precursors to various spacer functionalities. *J Org Chem*. 2000;65(4):958-963. https://doi.org/10.1021/jo9909554.
22 Yang J, Xiong Z, Chen Y, et al. The enantioselective synthesis of (+)-selina-3,11-dien-9-ol. *Synth Commun*. 1997;27(17):2985-2991. https://doi.org/10.1080/00397919708005005.
23 Yu WS, Jin ZD. A new strategy for the stereoselective introduction of steroid side chain viar-alkoxy vinyl cuprates: total synthesis of a highly potent antitumor natural product OSW-1. *J Am Chem Soc*. 2001;123(14):3369-3370. https://doi.org/10.1021/ja004098t.
24 Douelle F, Capes AS, Greaney MF. Highly diastereoselective synthesis of vicinal quaternary and tertiary stereocenters using the iodo-aldol cyclization. *Org Lett*. 2007;9(10):1931-1934. https://doi.org/10.1021/ol070482k.
25 Grimblat N, Zanardi MM, Sarotti AM. Beyond DP4: an improved probability for the stereochemical assignment of isomeric compounds using quantum chemical calculations of NMR shifts. *J Org Chem*. 2015;80(24):12526-12534. https://doi.org/10.1021/acs.joc.5b02396.
26 Zanardi MM, Sarotti AM. Sensitivity analysis of DP4+ with the probability distribution terms: development of a universal and customizable method. *J Org Chem*. 2021;86(12):8544-8548. https://doi.org/10.1021/acs.joc.1c00987.
27 Peng F, Tee JK, Setyawati MI, et al. Inorganic nanomaterials as highly efficient inhibitors of cellular hepatic fibrosis. *ACS Appl Mater Inter*. 2018;10(38):31938-31946. https://doi.org/10.1021/acsami.8b10527.